

Dynamics of Dipolar Spinor Condensates

Rong Cheng, J.-Q. Liang, Yunbo Zhang

Department of Physics and Institute of Theoretical Physics,

Shanxi University, Taiyuan 030006, P. R. China

(Dated: March 23, 2024)

Abstract

We study the semiclassical dynamics of a spinor condensate with the magnetic dipole-dipole interaction included. The time evolution of the population imbalance and the relative phase among different spin components depends greatly on the relative strength of interactions as well as on the initial conditions. The interplay of spin exchange and dipole-dipole interaction makes it possible to manipulate the atomic population on different components, leading to the phenomena of spontaneous magnetization and macroscopic quantum self-trapping. Simple estimate demonstrates that these effects are accessible and controllable by modifying the geometry of the trapping potential.

PACS numbers: 03.75.Kk, 03.75.Mn, 03.75.Nt, 05.30.Jp

I. INTRODUCTION

One of the current experimental advances of considerable importance in the context of ultracold atoms is the demonstration of multi-component Bose-Einstein condensate (BEC). In particular several groups have created spinor condensates of ^{23}Na atoms [1] and ^{87}Rb atoms [2] by transferring spin polarized condensates into far-off-resonance optical dipole traps, where the spin degree of freedom becomes active and the spinor nature of the condensates is manifested. The spin-mixing dynamics and its dependence on the magnetic field have been investigated in detail for both spin-1 and spin-2 condensates in a number of theoretical [3] and experimental works [1, 2]. Since the spin degree of freedom becomes accessible in an optical trap, the magnetic dipole-dipole interactions (MDDI) which arise from intrinsic or induced field of magnetic dipole moment [4, 5] should be taken into account in addition to the isotropic s-wave contact interaction. Due to their long-range and vectorial characters, the MDDI may largely enrich the variety of phenomena observed in condensates. Therefore this opens up new directions of research, such as the ground-state structure of spin-1 dipolar condensates in a single trap [6] as well as the ground-state magnetic properties of spinor BEC confined in deep optical lattices [7, 8, 9], where only the dipolar interactions between condensates at different sites are considered. Recently, a beautiful experiment in Stuttgart [10] has demonstrated BEC in a gas of chromium atoms ^{52}Cr , the MDDI of which is a factor of 36 higher than that for alkali atoms. This achievement makes possible the studies of the anisotropic long-range interactions in degenerate quantum gases.

The present paper exploits semiclassical dynamics of spin-1 dipolar condensates in a single trap and shows the time evolutions of the population imbalance and the relative phase among different spin components [6, 11]. This study may help us gain some insights into the properties of this dipolar spinor condensate, such as quantum phase diffusion, spontaneous magnetization [12] and Macroscopic Quantum Self Trapping (MQST). Especially, MQST known as a novel nonlinear effect has already been predicted theoretically [13] and very recently observed experimentally in double-well trap [14] and periodic optical lattice [15]. The selftrapping effect sustains a self-maintained interwell population imbalance during the nonlinear tunneling process. Here we will show that for a dipolar condensate the interplay between spin-exchange and MDDI gives rise to the intercomponent MQST naturally. Moreover, due to the adjustability of the MDDI, the experimental observation of the MQST effect

in dipolar spinor condensates can be expected.

The paper is organized as follows. In Sec. II we describe the dipolar spinor BEC model and derive the equations of motion of semiclassical dynamics in terms of symmetry. Sec. III is devoted to the properties of the equations of motion such as spontaneous magnetization and spin-mixing dynamics. The time evolutions of the population imbalance and the relative phase among different spin components are investigated and quantum tunneling and self-trapping among different spin components are examined carefully. Finally, a brief summary is given in Sec. IV.

II. THE MODEL AND THE EQUATIONS OF MOTION

We consider a spin $F = 1$ dipolar condensate with N bosons. In second quantized form, the Hamiltonian \hat{H}_{tot} subject to both spin-exchanging collisions \hat{H}_{sp} and MDDI \hat{H}_{dd} reads [6]

$$\hat{H}_{\text{tot}} = \hat{H}_{\text{sp}} + \hat{H}_{\text{dd}}$$

with

$$\begin{aligned} \hat{H}_{\text{sp}} = & \int d\mathbf{r} b^\dagger(\mathbf{r}) \left[\frac{5}{2M} + V_T(\mathbf{r}) \right] b(\mathbf{r}) \\ & + \frac{C_0}{2} \int d\mathbf{r} b^\dagger(\mathbf{r}) b^\dagger(\mathbf{r}) b(\mathbf{r}) b(\mathbf{r}) \\ & + \frac{C_2}{2} \int d\mathbf{r} b^\dagger(\mathbf{r}) b^\dagger(\mathbf{r}) F_{\alpha\beta} F_{\alpha\beta} b_{\alpha}(\mathbf{r}) b_{\beta}(\mathbf{r}) \end{aligned} \quad (1)$$

and

$$\begin{aligned} \hat{H}_{\text{dd}} = & \frac{C_d}{2} \int d\mathbf{r} \int d\mathbf{r}^0 \frac{1}{|\mathbf{r} - \mathbf{r}^0|^3} \\ & [b^\dagger(\mathbf{r}) b^\dagger(\mathbf{r}^0) F_{\alpha\beta} F_{\alpha\beta} b_{\alpha}(\mathbf{r}) b_{\beta}(\mathbf{r}^0) \\ & + b^\dagger(\mathbf{r}) b^\dagger(\mathbf{r}^0) (F_{\alpha\beta} - e)(F_{\alpha\beta} - e) b_{\alpha}(\mathbf{r}) b_{\beta}(\mathbf{r}^0)]; \end{aligned} \quad (2)$$

where $b_{\alpha}(\mathbf{r})$ ($\alpha = 0, \pm 1$) are the field annihilation operators for an atom in the hyperfine state $F = 1; m_F = \alpha$. The hyperfine spin F of one single atom is expressed in the spin-1 matrix representation, and M is the mass of the atom. A summation over repeated indices is assumed in Eqs. (1) and (2). The external trapping potential $V_T(\mathbf{r})$ is spin independent

for a far off-resonant optical dipole trap which makes atomic spin degree of freedom completely accessible. The two coefficients $c_0 = 4\pi\hbar^2(a_0 + 2a_2)/3M$, $c_2 = 4\pi\hbar^2(a_2 - a_0)/3M$ characterize the density-density and spin-spin collisional interactions, respectively, with a_f ($f = 0, 2$) being the s-wave scattering length for two spin-1 atoms in the combined symmetric channel of total spin f . And the dipolar interaction parameter is $c_d = \mu_B^2 g_F^2 / 4$ with g_F being the Landé g-factor, μ_B the Bohr magneton. $\mathbf{e} = (\mathbf{r} - \mathbf{r}')/|\mathbf{r} - \mathbf{r}'|$ is a unit vector. For the two experimentally created spinor condensates (^{23}Na and ^{87}Rb), we have $|\mathbf{c}_2| \ll c_0$:

For a condensate with its symmetry axis chosen to be along the quantization axis z (which happens to be the most experimentally relevant cases), \hat{H}_{dd} takes a very simple form as shown in Ref. [6]. Under the single mode approximation (SMA), namely, $\hat{\psi}(\mathbf{r}) = \psi(\mathbf{r})\hat{b}$; where $\psi(\mathbf{r})$ is the spin-independent condensate spatial wave function, \hat{b} is the annihilation operator for $m_F = 0$ component, the total Hamiltonian apart from a trivial term is given as

$$\begin{aligned} \hat{H}_{\text{tot}} = \hat{H}_{\text{sp}} + \hat{H}_{\text{dd}} = & \int d\mathbf{r} \hat{b}^\dagger \hat{b} + U_0 \int d\mathbf{r} \hat{b}^\dagger \hat{b} \hat{b}^\dagger \hat{b} \\ & + U_2 (\hat{b}_1^\dagger \hat{b}_1^\dagger \hat{b}_1 \hat{b}_1 + \hat{b}_1^\dagger \hat{b}_1^\dagger \hat{b}_1 \hat{b}_1 + 2\hat{b}_1^\dagger \hat{b}_1^\dagger \hat{b}_1 \hat{b}_1 \\ & + 2\hat{b}_1^\dagger \hat{b}_0^\dagger \hat{b}_1 \hat{b}_0 + 2\hat{b}_1^\dagger \hat{b}_0^\dagger \hat{b}_1 \hat{b}_0 + 2\hat{b}_0^\dagger \hat{b}_0^\dagger \hat{b}_1 \hat{b}_1 + 2\hat{b}_1^\dagger \hat{b}_0^\dagger \hat{b}_0 \hat{b}_0) \\ & + U_d (2\hat{b}_1^\dagger \hat{b}_1^\dagger \hat{b}_1 \hat{b}_1 + 2\hat{b}_1^\dagger \hat{b}_1^\dagger \hat{b}_1 \hat{b}_1 + 4\hat{b}_1^\dagger \hat{b}_1^\dagger \hat{b}_1 \hat{b}_1 \\ & + 2\hat{b}_1^\dagger \hat{b}_0^\dagger \hat{b}_1 \hat{b}_0 + 2\hat{b}_1^\dagger \hat{b}_0^\dagger \hat{b}_1 \hat{b}_0 + 2\hat{b}_0^\dagger \hat{b}_0^\dagger \hat{b}_1 \hat{b}_1 \\ & + 2\hat{b}_1^\dagger \hat{b}_1^\dagger \hat{b}_0 \hat{b}_0 + \hat{b}_1^\dagger \hat{b}_1 + \hat{b}_1^\dagger \hat{b}_1 + 2\hat{b}_0^\dagger \hat{b}_0); \end{aligned} \quad (3)$$

where $\int d\mathbf{r} \psi^2(\mathbf{r}) [5^2 = 2M + V_T(\mathbf{r})]$ (ψ is assumed to be of the same value for all components). $U_{0,2} = (c_{0,2}/2) \int d\mathbf{r} \psi^4(\mathbf{r})$ characterizes the spin-changing collisions and $U_d = (c_d/4) \int d\mathbf{r} d\mathbf{r}' \psi^2(\mathbf{r}) \psi^2(\mathbf{r}') (1 - 3\cos^2\theta_e) = \int d\mathbf{r} d\mathbf{r}' \psi^2(\mathbf{r}) \psi^2(\mathbf{r}') \mathbf{e} \cdot \mathbf{e}$ denotes the MDDI with θ_e being the polar angle of $(\mathbf{r} - \mathbf{r}')$. Before we proceed to examine the semiclassical dynamics of \hat{H}_{tot} ; we would like to emphasize that \hat{H}_{sp} is invariant under spin rotation, i.e., it possesses a $SO(3)$ symmetry in spin space [16]. The presence of the MDDI breaks this symmetry into $SO(2)$, which means \hat{H}_{tot} has only axial symmetry in spin space as we chosen the quantization axis along z . In this sense the MDDI plays a similar role to that of an external magnetic field.

In the mean-field theory the condensate is usually considered to be in a coherent state [11]

$$|j\rangle_i = \exp\left\{-\frac{1}{2} \sum_j |z_j|^2\right\} \exp\left\{\sum_j z_j b_j^\dagger\right\} |0\rangle_i; \quad (4)$$

where $|0\rangle_i$ is the vacuum state. The complex numbers z_j are nothing but the macroscopic wave functions for the atoms in the hyperfine level $F = 1; m_F = -1$ with population N and phase θ ; i.e.,

$$z_j = \sqrt{\frac{P}{N}} e^{i\theta_j}; \quad (5)$$

The time-dependent variational principle of the system

$$S = \int_0^T \langle i | \hbar \dot{z}^\dagger | j \rangle \langle j | \dot{z} | i \rangle - \hbar z^\dagger H | j \rangle \langle j | z | i \rangle dt = 0 \quad (6)$$

gives rise to the Hamiltonian equations of motion in complex coordinates

$$i\hbar \dot{z} = \frac{\partial H_0}{\partial z^\dagger}; \quad i\hbar \dot{z}^\dagger = \frac{\partial H_0}{\partial z} \quad (7)$$

with

$$H_0(N; \theta) = (\mu + U_d)N - 3U_d N_0 + U_0 N^2 + (U_2 + 2U_d)(N_1 - N_{-1})^2 + 2(U_2 - U_d)N_0 N_1 + N_{-1} + 2\sqrt{\frac{P}{N_1 N_{-1}}} \cos(2\theta_0 - \theta_1 - \theta_{-1}); \quad (8)$$

Note that the dynamics governed by Hamiltonian (3) conserves the total atom numbers $N = \sum_P N_P$ and the total hyperfine spin of the condensate in the direction of the quantization axis $I = (N_1 - N_{-1})/\hbar$. In terms of the following canonical variables

$$\begin{aligned} \phi_1 &= \frac{(\theta_1 + \theta_0 - \theta_{-1})}{3} & n_1 &= N_1 + N_0 + N_{-1} \\ \phi_2 &= \theta_0 - \frac{(\theta_1 + \theta_{-1})}{2} & \text{and } n_2 &= \frac{2}{3}N_0 - \frac{1}{3}(N_1 + N_{-1}) \\ \phi_3 &= \theta_1 - \theta_{-1} & n_3 &= \frac{(N_1 - N_{-1})}{2} \end{aligned} \quad (9)$$

the Hamiltonian (8) becomes cyclic in the coordinates ϕ_1 and ϕ_3

$$\begin{aligned} H_0(\phi_1; \phi_2; \phi_3; n_2) &= \mu n_1 + U_0 \frac{n_1^2}{3} - 3U_d n_2 \\ &+ 4(U_2 + 2U_d) \frac{n_2^2}{3} + 2(U_2 - U_d) \\ &\times \left[\frac{1}{3} n_1 + n_2 - \frac{2}{3} n_1 - n_2 \right. \\ &+ \left. \frac{2}{3} n_1 - n_2 - 4 \frac{n_2^2}{3} - \frac{1}{3} n_1 + n_2 \cos 2\phi_2 \right]; \end{aligned} \quad (10)$$

Two important consequences follow as a result of the cyclic coordinates ϕ_1 and ϕ_3 : Firstly the mean value of the total number of atoms $N = n_1$ and that of the total hyperfine spin of the condensate $I = 2n_3$ are constants of motion. The dynamics, on the other hand, involves only one pair of variables $\phi_2; p_2$ as

$$p_2 = \frac{\partial H_0}{\partial \phi_2}; \quad \phi_2 = \frac{\partial H_0}{\partial p_2};$$

Define $n_i = n_i/N$ ($i = 1; 2; 3$) and $\phi = \frac{1}{N} \frac{1}{(\frac{2}{3} \phi_2)^2 + 4 \frac{2}{3}}$, we obtain

$$\begin{aligned} \phi_2 &= 4N (U_2 - U_d) \left[\frac{1}{3} + \phi \sin 2\phi_2 \right] \\ \phi_2 &= 3U_d + 2N (U_2 - U_d) \left[2\phi_2 \frac{1}{3} \right. \\ &\quad \left. + 2N (U_2 - U_d) \frac{\frac{2}{3} \phi_2^2 + 2\phi_2 \frac{1}{3} + 4 \frac{2}{3}}{\cos 2\phi_2} \right] \end{aligned} \quad (11)$$

That means not only ϕ_2 but also ϕ_3 are involved in the dynamics.

The variables ϕ_2 and p_2 are canonically conjugate in a classical Hamiltonian

$$\begin{aligned} H &= \frac{(U_2 - U_d)N}{2} \phi_2^2 + \frac{1}{3} \phi_2^3 \\ &\quad + 2(U_2 - U_d)N \left[\frac{1}{3} \phi_2 + \phi \cos 2\phi_2 \right] - 3U_d \phi_2 \end{aligned} \quad (12)$$

In a simple mechanical analogy, H describes a nonrigid pendulum. The Bose Josephson junction (BJJ) tunneling current between different spin components is given by

$$I_{BJJ} = \frac{\partial H}{\partial \phi_2} = I_0 \left[\frac{1}{3} + \phi \sin 2\phi_2 \right]; \quad (13)$$

where $I_0 = 2N^2 (U_2 - U_d)$. It differs from BJJ tunneling current of two weakly linked BEC in a double-well potential in its further nonlinearity in ϕ_2 [13].

III. PROPERTIES OF THE EQUATIONS OF MOTION

A. Spontaneous magnetization

We firstly study the equilibrium configurations of the system. They are determined by the classical equations of motion (11) after setting the time derivative terms to zero

$$0 = \frac{1}{3} + \frac{1}{2} \sin 2\theta_2 \quad (14)$$

$$0 = \frac{1}{3} \left[\frac{2}{3} \frac{1}{2} \frac{1}{3} + \frac{4}{3} \cos 2\theta_2 \right] \quad (15)$$

We have defined a dimensionless parameter $\eta = \frac{3U_d}{2J_2 U_d N}$ characterizing the relative interaction strength of the MDDI. In Eq. (15) plus sign corresponds to the case of $(U_2 - U_d) > 0$; while minus sign corresponds to $(U_2 - U_d) < 0$ (In the following we take the former case as an example): From the definition of η we know that the constant of motion η takes values in the interval $\frac{1}{2} < \eta < \frac{1}{2}$ and the dynamic variable θ_2 in the interval $\frac{1}{3} < \theta_2 < \frac{2}{3} - 2j_3j$. In the following discussion about the solutions of the equilibrium equations we separately consider three cases in order to see more clearly how these solutions depend on the relative phase θ_2 .

(1) Equilibrium configuration with $\cos 2\theta_2 = 1$ (or $2\theta_2 = 2k\pi$):

The equilibrium value of θ_2 is thus given by equation (15) with $\cos 2\theta_2 = 1$; which has only one solution in the interval $\frac{1}{3} < \theta_2 < \frac{2}{3} - 2j_3j$. When $\eta = 1$ the equilibrium value of θ_2 approaches its upper boundary $\frac{2}{3} - 2j_3j$. In this case the fractions of atoms $n = N^{-1}N_i$ ($i = 0, 1$) occupying three hyperfine states are $n_1 = j_3j + \frac{1}{3}$; $n_0 = \frac{1}{3} - 2j_3j$; $n_1 = j_3j - \frac{1}{3}$. On the other hand when $\eta = \frac{1}{2}$ θ_2 is at the lower boundary $\frac{1}{3}$; where the fractions of atoms occupying the hyperfine states are $n_1 = \frac{1}{2}(1 + 2j_3)$; $n_0 = 0$; $n_1 = \frac{1}{2}(1 - 2j_3)$. Besides, when $j_3 = 0$ the equilibrium value of θ_2 is $\theta_2 = \frac{1}{2}$ in the interval $\frac{1}{3} < \theta_2 < \frac{2}{3}$ and the occupation fractions of three hyperfine states are respectively $n_0 = \frac{1}{2}(1 - \eta)$; $n_1 = n_{-1} = \frac{1}{4}(1 + \eta)$:

(2) Equilibrium configuration with $\cos 2\theta_2 = -1$ (or $2\theta_2 = (2k+1)\pi$):

Now the equilibrium value of θ_2 is given by equation (15) with $\cos 2\theta_2 = -1$. Similarly it has again only one solution in the interval $\frac{1}{3} < \theta_2 < \frac{2}{3} - 2j_3j$. When $\eta = 1$ $\theta_2 = \frac{1}{3}$;

θ_2 is at the lower boundary $\theta_2 = \frac{\pi}{3}$: In particular, when $\theta_3 = 0$ the solution only exists for vanished dipole-dipole interaction U_d .

(3) Equilibrium configuration with $\cos 2\theta_2 = 0$ (or Equilibrium configuration which does not depend on the phase θ_2).

In this case there exist two solutions which are independent of the value of θ_3 : One solution appears at the lower boundary $\theta_2 = \frac{\pi}{3}$ and the occupation fractions are $n_1 = n_2 = \frac{1}{2}$; $n_0 = 0$: The other one appears at the upper boundary $\theta_2 = \frac{2\pi}{3}$ and the occupation fractions are $n_1 = n_2 = \frac{1}{2}$; $n_0 = 0$: Interestingly when $\theta_3 = 0$ the occupation fractions become $n_1 = n_2 = 0$ and $n_0 = 1$; corresponding to the "polar" state of the condensate.

The mean field theory predicted a polar ground state of spinor BEC for ^{23}Na in which the atoms interact antiferromagnetically with each other in the absence of the MDDI [16]. The intrinsic magnetic moment of particles may, however, contribute together to form a Bose-Einstein Ferromagnetism (BEF) [12]. Spinor bosons carry magnetic moments and $M = \hbar j_1 j_2$ represents the magnetization. Spontaneous magnetization means that M remains finite even if the external magnetic field B vanishes, namely, the ground state of spinor BEC is always ferromagnetic state. Our calculations prefer the latter scenario. Specifically, above results suggest that for most given values of θ_3 and initial relative phase among the three components, when $B = 0$ and $U_2 > 0$; we have $M \neq 0$, i.e., the system is magnetized spontaneously once the dipolar spinor BEC is realized. As mentioned in Ref. [12], one can provide a direct way of confirming spontaneous magnetization experimentally. Considering that both the sign and the magnitude of the MDDI coefficient c_d depend on the geometric shape of the condensate [4, 10, 17, 18], we can conveniently adjust the trap aspect ratio to manipulate the magnetic property of its ground state.

B. Spin-Mixing Dynamics

A key feature of dipolar spinor BEC is that besides the usual two-body repulsive hard-core interactions, there also exist spin-exchange interaction and MDDI which lead to spin mixing within the condensates. Population can be transferred from one spin state to another under internal nonlinear interactions without the presence of external fields. Insight into the complex dynamics of our system can be gained by employing the method of action-angle

variables [19]. In the subsequent section we present some numerical results and show the time evolutions of the population imbalance and the relative phase among different spin components for two cases a) $\beta_3 = 0$ and b) $\beta_3 \neq 0$; i.e., whether total hyperfine spin of the condensate is zero or not. Time has been rescaled in units of $2J_2/U_d N \approx$ in Figures 1 and 2.

Figure 1 shows solutions of the population imbalance and relative phase of Eqs. (11) with initial conditions $\beta_2(0) = 0.12$; $\beta_3(0) = 0.25$; $\beta'_2(0) = \frac{\pi}{2}$ for the relative interaction parameters $\beta = \frac{3U_d}{2J_2 U_d N} = 0.00; 0.40; 0.60$ and 0.75 , respectively. The left column exhibits the time evolutions of the population imbalance between 0 and ± 1 components. Josephson sinusoidal oscillations are observed as β increases in Figs. 1a, 1b. In Fig. 1c, there is a critical transition point for $\beta = \beta_c = 0.60$. Increasing β further for example to $\beta = 0.75$, the population of each equivalent component oscillates around a nonzero time averaged value, which gives a net population imbalance $\langle \beta_2(t) \rangle > 0$. This is closely related to the MQST phenomenon. Simultaneously, the right column shows the time evolutions of the relative phase between 0 and ± 1 components and indicates that as β increases $\beta'_2(t)$ varies from a monotonically increasing function of time to a periodically oscillating function of time. In the nonrigid pendulum analogy, this corresponds that the motion of our system is turned from "running-phase modes" (Figure 1a) into "phase modes" (Figures 1b-1d) or from a rotation into a vibration. Here the definitions of running-phase modes and phase modes are the same as those for two weakly coupled BEC [14].

This critical behavior depends on $\beta_c = \beta_c(\beta_2(0); \beta_3(0); \beta'_2(0) = \frac{\pi}{2})$, as can be easily found from the energy conservation constraint and the boundness of the tunneling energy in Eq. (12). In fact, the value $\langle \beta_2(t) \rangle < 0$ is inaccessible at any time if

$$\beta_c = \frac{1}{3} \beta_2(0) + \frac{\frac{1}{2} \sqrt{1 - 9\beta_3^2(0)}}{9\beta_2(0)} \frac{(1 + 3\beta_2(0)) \sqrt{(2 - 3\beta_2(0))^2 - 36\beta_3^2(0)}}{9\beta_2(0)}; \quad (16)$$

When $\beta'_2(0) = 0$ the critical parameter is

$$\beta_c = \frac{1}{3} \beta_2(0) + \frac{\frac{1}{2} \sqrt{1 - 9\beta_3^2(0)}}{9\beta_2(0)} \frac{(1 + 3\beta_2(0)) \sqrt{(2 - 3\beta_2(0))^2 - 36\beta_3^2(0)}}{9\beta_2(0)}; \quad (17)$$

and $\kappa < \kappa_c$ marks the regime of MQST. Specifically for $n_2(0) = 0.12$; $n_3(0) = 0.25$; the critical parameter is $\kappa_c = 0.18$. We take $\gamma = 0.20$ and see MQST does set in.

In Figure 2 we show solutions of Eqs. (11) with initial conditions $n_2(0) = 0.12$; $n_3(0) = 0$; $\phi_2(0) = 0$ for parameters $\gamma = 0.75; 0.60; 0.43$ and 0.00 ; respectively. The left column shows again the time evolutions of the population imbalance between 0 and 1 components and indicates that $n_2(t)$ is always a periodic function of time as κ decreases. For $\kappa = \kappa_c = 0.43$ the population difference is self locked to the initial value, which serves as another sign of the MQST phenomenon. The right column shows the time evolution of the relative phase between 0 and 1 components and indicates that as κ decreases $\phi_2(t)$ is always a periodic function of time around its mean value $\langle \phi_2(t) \rangle = 0$. The dynamics corresponds to "zero-phase modes". Moreover we observe that MQST occurs when

$$\kappa < \kappa_c = \frac{2}{3} n_2(0); \quad (18)$$

while for $\phi_2(0) = \pi$ MQST never happens.

Therefore it is obvious that the spin-mixing dynamics depends on the relative interaction parameter κ and is also sensitive to the initial occupations and relative phases of the three components, which can be adjusted by engineering Raman pulses [20]. In practical experiments there are usually two different ways to achieve MQST. In Figures 1 and 2, $n_2(0)$ and $\phi_2(0)$ are kept constants while κ varies (by changing the geometry of condensates). On the other hand, one can calibrate the initial values of the population imbalance $n_2(0)$ with a fixed trap geometry (i.e., κ remains constant) and $\phi_2(0)$ [15].

In order to further characterize the evolution of the system we summarize the full dynamic behavior of Eq. (11) in Figure 3 that shows the $n_2(t)$ - $\phi_2(t)$ phase portrait with constant energy contour. The distinction between the two dynamic regimes { nonlinear Josephson tunneling and MQST } becomes more apparent in Figure 3. In the regime of Josephson oscillation the dynamic variables follow a closed phase space trajectory, while in the self-trapping regime they follow an open trajectory with an unbounded phase.

We are inspired by the great expectation that tuning the contact interaction between cold atoms close to zero by Feshbach resonance [21] will make the MDDI more prominent or even the dominant interaction [10]. Based on the experimental values of the s-wave scattering lengths for ^{23}Na , $a_0 = (50.0 \pm 1.6) a_B$ and $a_2 = (55.0 \pm 1.7) a_B$ with a_B being the Bohr radius [23], the ratio of coefficients c_d and $|j_2|$ can be shown to be 0.007, while for

^{87}Rb ($a_0 = 101.8a_B$ and $a_2 = 100.4a_B$) it is 0.1 [6]. Evaluation with a simple variational wave function [24] gives $U_2 N \sim 6nK$ for a sodium condensate up to $N = 5 \times 10^6$ atoms confined in an optical dipole trap with a very small trapping volume (10^{-8} cm^3) [1, 22]. On the other hand, as argued in Refs. [4, 6, 10, 17, 18], both the sign and the magnitude of the MDDI U_d can be greatly tuned with trapping geometry. As has been shown [6], $U_d=U_2$ depends on a monotonically increasing function of the condensate aspect ratio, bounded between 1 and 2. This clearly shows the possibility of adjusting the MDDI very close to spin exchange interaction, i.e. $U_d=U_2 \sim 1$. At this point our parameter may take values in a large scale and the manifestation of MQST is within reach with current technologies. We point out although for all of the alkali-metal atomic condensations the MDDI is rather weak compared to the contact potential, the experimental achievement of BEC with transition-metal chromium ^{52}Cr provides us the hope because the MDDI here is 36 times stronger than that of alkali atoms. For these reasons, a degenerate quantum gas with adjustable long- and short-range interactions can be experimentally realized in near future. By altering the strengths of two kinds of interactions and the initial conditions, the nonlinear tunneling dynamics of dipolar spinor BEC consequently sustains a self-maintained population imbalance: a novel MQST effect. Such a scheme would avoid the difficulty of realizing experimentally the double-well magnetic trap.

IV. SUMMARY

In summary we have described a semiclassical treatment of the spin-1 dipolar spinor condensates. As a result of the conservation of atom numbers and total hyperfine spin of the condensate, the classical equations of motion are derived and discussed in a similar way as in double-well BJJ. It is demonstrated that spontaneous magnetization and spin-mixing dynamics depend on both the spin-exchange interaction U_2 and the MDDI U_d through the ratio $\frac{3U_d}{2U_2 U_d N}$. The initial population imbalance, the relative phase among the three components of the condensate as well as the total hyperfine spin of the system all play important roles in the semiclassical dynamics. Finally we have indicated the possibility of using dipolar spinor condensate as a platform for practical manipulation of MQST and Josephson oscillation.

V . ACKNOWLEDGMENT

This work was supported by National Natural Science Foundation of China under Grant Nos.10475053, 10175039 and 90203007.

* corresponding author: ybzhang@sxu.edu.cn

-
- [1] D . M . Stamper-K um, M . R . Andrews, A . P . Chikkatur, S . Inouye, H .-J . M iesner, J . Stenger, and W . K etterle, Phys. Rev. Lett. 80, 2027 (1998); J . Stenger, S . Inouye, D . M . Stam per-K um, H .-J . M iesner, A . P . Chikkatur and W . K etterle, Nature 396, 345 (1998).
 - [2] H . Schm alphann, M . Erhard, J . K ronjäger, M . K ottke, S . van Staa, L . Cacciapuoti, J . J . Arlt, K . Bongs, and K . Sengstock, Phys. Rev. Lett. 92, 040402 (2003); M .-S . Chang, C . D . Ham ley, M . D . Barrett, J . A . Sauer, K M . Fortier, W . Zhang, L . You, and M . S . Chapm an, Phys. Rev. Lett. 92, 140403 (2004); T . Kuwamoto, K . Araki, T . Eno, and T . Hirano, Phys. Rev. A 69, 063604 (2004); J . M . Higbie, L . E . Sadler, S . Inouye, A . P . Chikkatur, S . R . Leslie, K . L . Moore, V . Savalli, D . M . Stam per-K um, cond-m at/0502517.
 - [3] C . K . Law , H . Pu, and N . P . Bigelow , Phys. Rev. Lett. 81, 5257 (1998); H . Pu, C . K . Law , S . Raghavan, J . H . Eberly, and N . P . Bigelow , Phys. Rev. A 60, 1463 (1999); Hiroki Saito, Masahito Ueda, cond-m at/0504398; Wenxian Zhang, D . L . Zhou, M .-S . Chang, M . S . Chapman, L . You, cond-m at/0502061.
 - [4] S . Yi and L . You, Phys. Rev. A 61, 041604 (R) (2000); S . Yi and L . You, Phys. Rev. A 63, 053607 (2001).
 - [5] K . Goral, K . R zaszewski, and T . Pfau, Phys. Rev. A 61, 051601 (R) (2000).
 - [6] S . Yi, L . You, and H . Pu, Phys. Rev. Lett. 93, 040403 (2004).
 - [7] H . Pu, W .-P . Zhang, and P . M eystre, Phys. Rev. Lett. 87, 140405 (2001).
 - [8] W .-P . Zhang, H . Pu, C . P . Search, and P . M eystre, Phys. Rev. Lett. 88, 060401 (2002).
 - [9] K . Gross, C . P . Search, H . Pu, W .-P . Zhang, and P . M eystre, Phys. Rev. A 66, 033603 (2002).
 - [10] A . Griesm aier, J . W erner, S . Hensler, J . Stuhler, and T . P fau, Phys. Rev. Lett. 94, 160401 (2005).
 - [11] D . R . Rom ano and E . J . V . de Passos, Phys. Rev. A 70, 043614 (2004).
 - [12] Q . Gu, Phys. Rev. A 68, 025601 (2003).

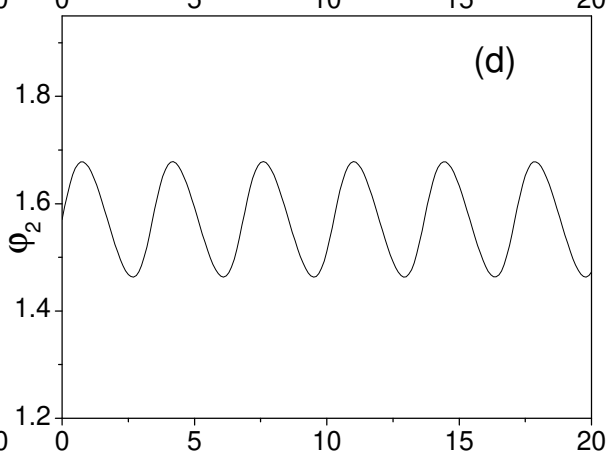
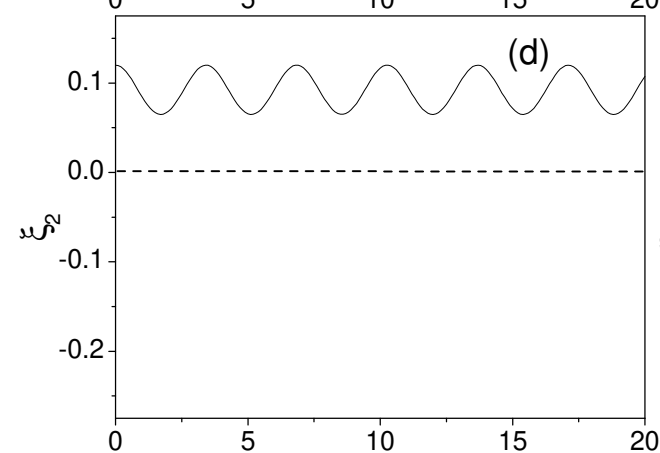
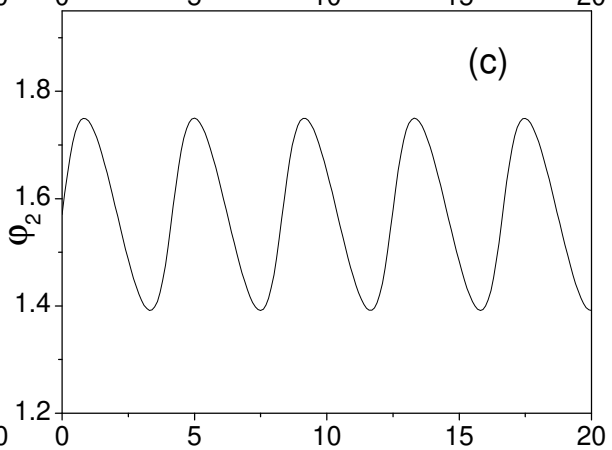
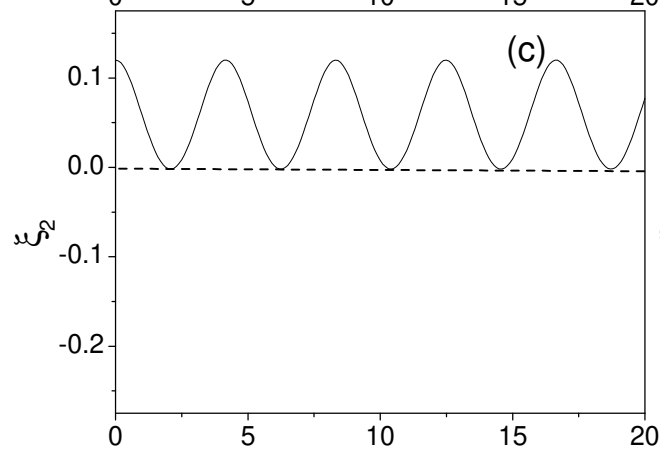
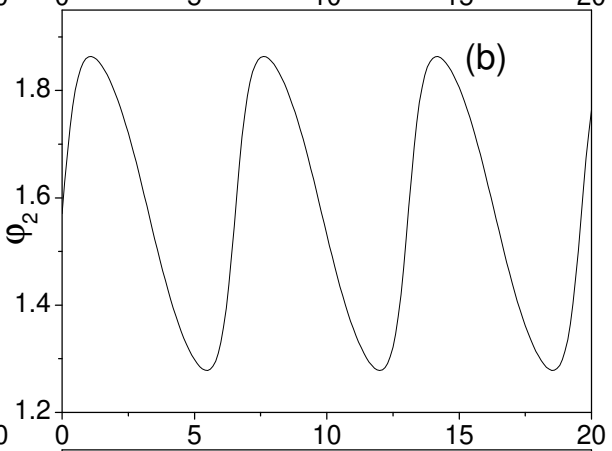
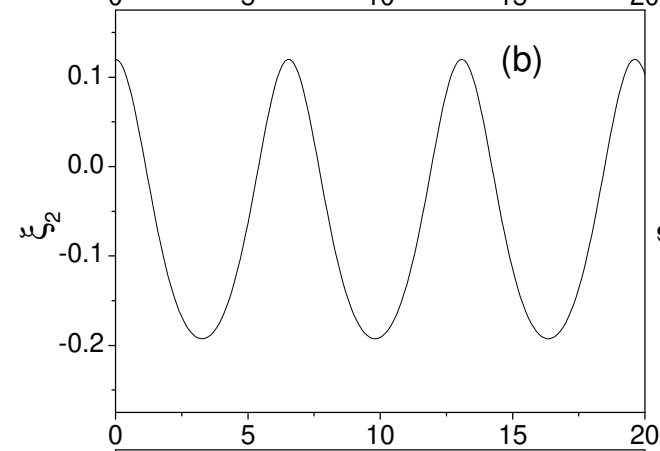
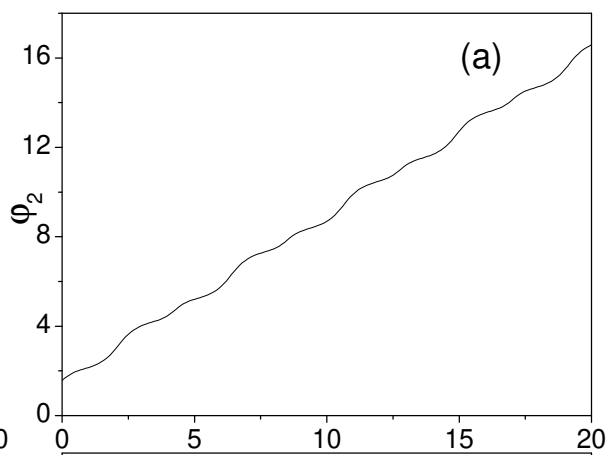
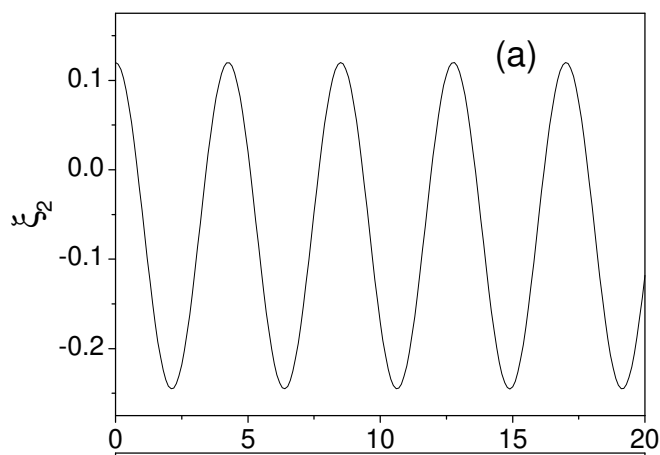
- [13] A . Sm erzi, S . Fantoni, S . G iovanazzi, and S . R . Shenoy, Phys. Rev. Lett. 79, 4950 (1997); S . Raghavan, A . Sm erzi, S . Fantoni, and S . R . Shenoy, Phys. Rev. A 59, 620 (1998).
- [14] M . A lbiez, R . G ati, J . F ølling, S . Hunsm ann, M . C ristani, and M . K . Oberthaler, cond-m at/0411757.
- [15] Th . Anker, M . A lbiez, R . G ati, S . Hunsm ann, B . E iem ann, A . Trom bettoni and M . K . Oberthaler, Phys. Rev. Lett. 94, 020403 (2005).
- [16] T . L . Ho, Phys. Rev. Lett. 81, 742 (1998).
- [17] C . Eberlein, S . G iovanazzi, and D . H . J . O 'D ell, cond-m at/0311100.
- [18] S . G iovanazzi, A . G orlitz, and T . P fau, Phys. Rev. Lett. 89, 130401 (2002).
- [19] J . G amier, F . K h . Abdullaev, cond-m at/0409479.
- [20] H . Pu, C . K . Law , and N . P . Bigelow , Physica B 280, 27 (2000).
- [21] E . T im m em ans, P . Tom m asini, M . Hussein, and A . K erm an, Physics Reports 315, 199 (1999).
- [22] K . B . Davis, M . O . M ewes, M . R . Andrews, N . J . van D ruten, D . S . D urfee, D . M . Kum, and W . K etterle, Phys. Rev. Lett. 75, 3969 (1998).
- [23] A . C rubellier, O . D ulieu, F . M asnou-Seeuws, M . E lls, H . K nockel, and E . T im ann, Eur. Phys. J. D 6, 211 (1999).
- [24] G . Baym and C . J . Pethick, Phys. Rev. Lett. 76, 6 (1996).

Figure Captions

Figure 1: Spin-M ixing Dynam ics: the population im balance ρ_2 and relative phase ϕ_2 versus time for initial conditions $\rho_2(0) = 0.12$; $\rho_3(0) = 0.25$; $\phi_2(0) = \frac{\pi}{2}$ and $\phi_3 = 0$ (a); 0.4 (b); 0.6 (c) and 0.75 (d). Time is rescaled in units of $2\hbar J_2 - U_d \hbar N \approx$:

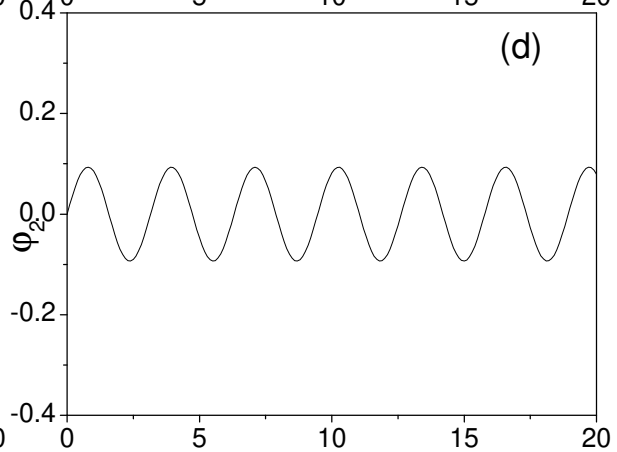
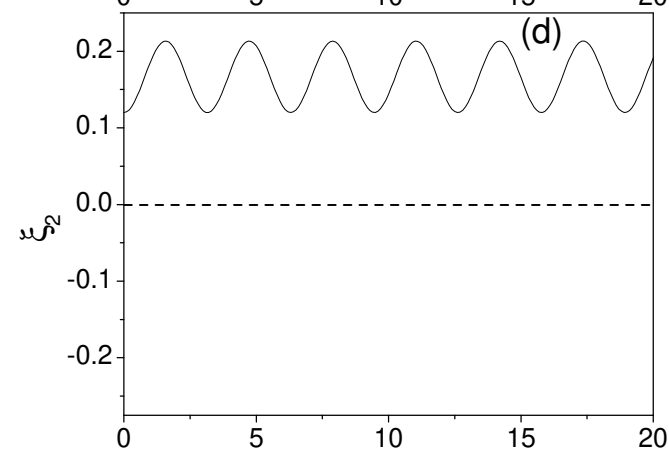
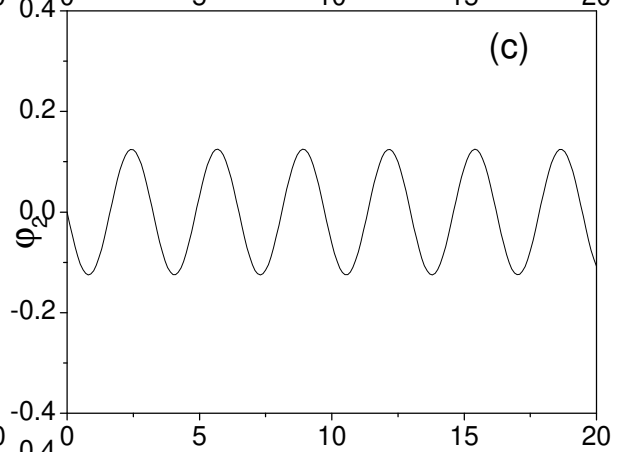
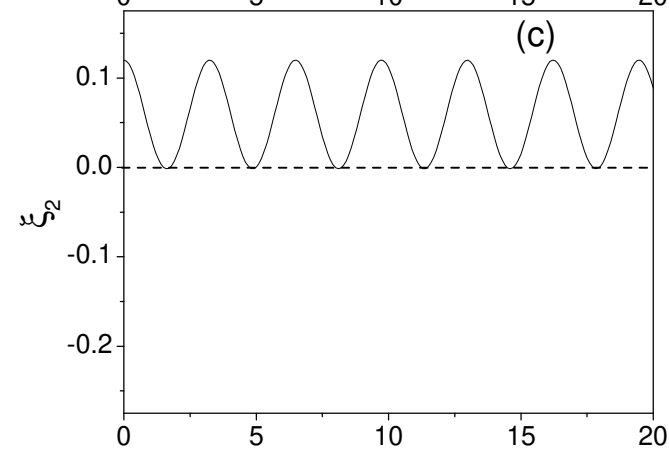
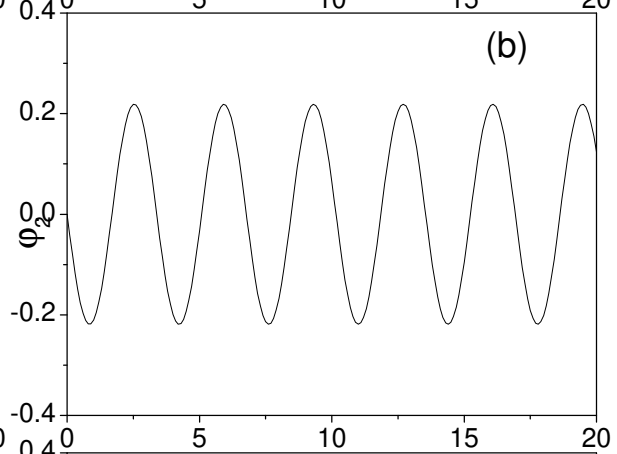
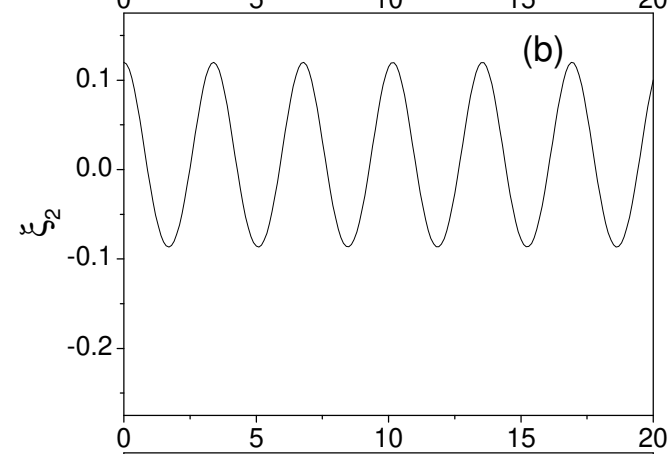
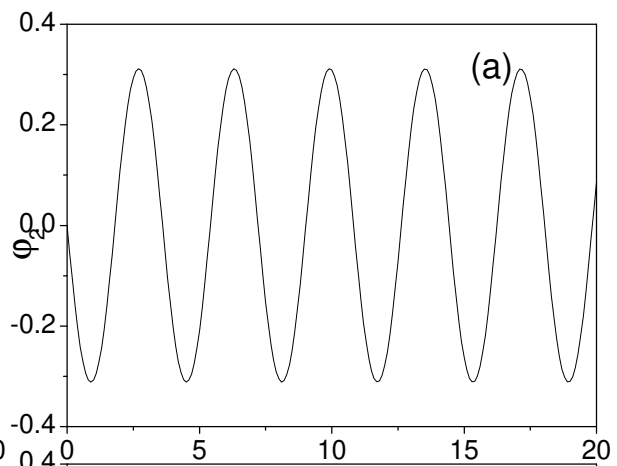
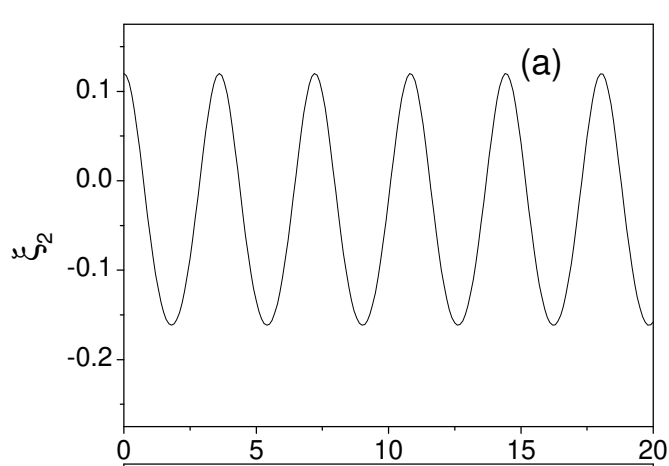
Figure 2: Same as in Figure 1 for initial conditions $\rho_2(0) = 0.12$; $\rho_3(0) = 0$; $\phi_2(0) = 0$ and $\phi_3 = 0.75$ (a); 0.6 (b); 0.43 (c) and 0 (d) :

Figure 3: Constant energy contours in a phase-space plot of population im balance ρ_2 versus phase di erence ϕ_2 . The upper panel: $\rho_3(0) = 0.25$ and $\phi_3 = 0.6$ ($c_2 > 0$). The lower panel: $\rho_3(0) = 0$ and $\phi_3 = 0.2$ ($c_2 < 0$). Dark areas mean lower energy.



time

time



time

time

